Ocean Modelling 39 (2011) 125–134

Contents lists available at ScienceDirect

Ocean Modelling

journal homepage: www.elsevier.com/locate/ocemod

An eddy closure for potential vorticity

Todd Ringler [a,*], Peter Gent [b]

[a] Theoretical Division, Los Alamos National Laboratory, Los Alamos, NM 87545, USA
[b] Climate and Global Dynamics, National Center for Atmospheric Research, Boulder, CO 80307, USA

ARTICLE INFO

Article history:
Available online 25 February 2011

Keywords:
Potential vorticity
Eddy-closure

ABSTRACT

It is now over 40 years since a closure for the effects of mesoscale eddies in terms of Ertel potential vorticity was first proposed. The consequences of the closure that treats potential vorticity exactly the same as a passive tracer in isopycnal coordinates are explored in this paper. This leads to a momentum equation to predict the mean velocity. While the momentum equation is not unique due to the presence of an undefined potential function, the total energy equation is used to constrain its functional form. The inviscid form of the proposed eddy closure nearly conserves total energy; the error in conservation of total energy is proportional to the time derivative of the bolus velocity. The proposed eddy closure retains Kelvin's circulation theorem with mean potential vorticity conserved along particle trajectories following the transport (mean + bolus) velocity field. The relative vorticity component of the potential vorticity being diffused along isopycnals leads to terms that look like viscous stress, but these terms do not satisfy two important conditions of standard viscous closures. A numerical model based on this closure is developed, and idealized simulations in a re-entrant zonal channel are conducted to evaluate the merit of the proposed closure. When comparing various eddy closures to an eddy-resolving reference solution, the closure that both transports and diffuses potential vorticity performs marginally better than its peers, particularly with respect to the core zonal jet structure and position. However, these favorable results are obtained only if a potential vorticity diffusion coefficient is used that is smaller than the coefficient used to compute the bolus velocity. Based on these results, we conjecture that extending eddy-closures to include potential vorticity dynamics is possible, but will require the use of a closure parameter that varies temporally and spatially.

© 2011 Elsevier Ltd. All rights reserved.

1. Introduction

The most widely used closure for the effects of ocean mesoscale eddies on the mean flow was proposed in Gent and McWilliams (1990); GM hereafter. GM changes the equations for potential temperature and salinity in z-coordinates, or the layer thickness and tracer equations in isopycnal coordinates. In virtually all ocean models and ocean components of climate models, the momentum equation used is just the usual primitive equation form for the mean velocity.

However, an idea that predates GM is that the eddy closure should be based on the Ertel potential vorticity (PV), as it is often considered the most fundamental dynamical variable because it satisfies the same conservation equation as a passive tracer. If an invertability principle is assumed, then all the other dynamical variables can be determined if the PV distribution is known. A PV closure was first discussed by Green (1970), Welander (1973), Marshall (1981), and in the homogenization theory of Rhines and Young (1982). More recently, it has been proposed in many papers, such as Killworth (1997), Greatbatch (1998), Smith (1999), Wardle and Marshall (2000), Plumb and Ferrari (2005), Eden (2010), and Marshall and Adcroft (2010). However, in most of these papers either the quasigeostrophic approximation is used, or the PV in the mixing term is approximated by its dominant term, the Coriolis parameter divided by the layer thickness. We think this second approximation is not justified because it is the full Ertel PV that satisfies the passive tracer equation, whereas the dominant PV term does not. This approximation eliminates the terms due to the relative vorticity in PV, which look like viscous terms in the momentum equation. In this paper, the consequences of an eddy closure based on the full Ertel PV are explored in detail. One consequence is that the eddy closure changes the vorticity equation and, hence, the momentum equation of the model.

Proposals based on PV have also been made for the form of the bolus, or eddy-induced, velocity that also advects tracers in the GM closure. For a constant coefficient, the Gent and McWilliams (1990) bolus velocity is based on the gradient of the layer thickness. Treguier et al. (1997) and Marshall et al. (1999) both propose instead to use the gradient of layer thickness divided by the Coriolis parameter, which is the inverse of the PV dominant term. Consequences of

* Corresponding author. Tel.: +1 505 667 7744.
E-mail address: ringler@lanl.gov (T. Ringler).

1463-5003/$ - see front matter © 2011 Elsevier Ltd. All rights reserved.
doi:10.1016/j.ocemod.2011.02.003

this form are that the GM property of an assured domain-averaged sink of potential energy is lost, and an additional term becomes very large near the equator and needs to be regularized.

In this paper, the closure that we develop assumes that mean Ertel PV should obey the same conservation equation as a passive tracer, which requires that it is a function of the mean velocity. Then the momentum equation must solve for the mean velocity, not the transport velocity which is the sum of the mean and bolus velocities. We propose a momentum equation that results in Ertel PV being conserved along particle trajectories defined by the transport velocity, just like a passive tracer. This proposal can be used with *any* chosen form for the bolus velocity. There have been previous proposals to use a different momentum equation in non-eddy-resolving models. Gent and McWilliams (1996) suggest that momentum advection should be by the transport velocity, not the mean velocity, to be consistent with the tracer advection. Smith (1999) proposed a different momentum equation for the mean velocity based on stochastic turbulence theory, but we are not aware that either form has been implemented in any ocean model. McDougall and McIntosh (1996) and Greatbatch (1998) both propose a more radical change; namely that the momentum equation should be written entirely in terms of the transport velocity. Numerical models using this form of momentum equation have been implemented, and used to obtain global solutions by Ferreira and Marshall (2006) and midlatitude solutions by Zhao and Vallis (2008). With this form of the momentum equation a mean PV is conserved, but it is a function of the transport velocity rather than the mean velocity, which cannot be justified theoretically.

Section 2 shows the new closure in terms of PV, Section 3 contains an analysis of energetics, and Section 4 is an analysis of the momentum equation that results from this PV closure. A set of re-entrant zonal channel simulations is discussed in Section 5 to compare and contrast some of the various eddy-closure approaches.

2. Potential vorticity mixing in isopycnal coordinates

2.1. The inviscid, adiabatic system

This analysis is done in isopycnal coordinates, because it is important to average along isopycnal surfaces of constant potential density, ρ, and use the incompressible, Bousinesq, adiabatic and hydrostatic equations of motion. The isopycnal layer thickness equation is

$$\frac{\partial h}{\partial t} + \nabla \cdot (h\mathbf{u}) = 0, \tag{1}$$

where the isopycnal layer thickness, h, is defined as $h = -\partial z/\partial \rho$ and z is the height of constant density surfaces. h is transported by the horizontal velocity $\mathbf{u}$. The along-isopycnal inviscid momentum equation can be written in the form

$$\frac{\partial \mathbf{u}}{\partial t} + (f + \zeta)\mathbf{k} \times \mathbf{u} + \nabla\phi + \nabla K = 0, \tag{2}$$

where ζ is the relative vorticity defined as $\zeta = \mathbf{k} \cdot \nabla \times \mathbf{u}$, $\mathbf{k}$ is the vertical unit vector, f is the Coriolis parameter, ϕ is the Montgomery potential, and K is the kinetic energy defined as $\frac{1}{2} \mid \mathbf{u} \cdot \mathbf{u} \mid .\phi = (p + g\rho z)/\rho_0$, where p is the pressure, g gravity, and ρ_0 a reference density. The absolute vorticity equation results from applying the $\mathbf{k} \cdot \nabla \times$ operator to (2) to obtain

$$\frac{\partial \omega}{\partial t} + \nabla \cdot (\omega\mathbf{u}) = 0, \tag{3}$$

where the absolute vorticity is defined as $\omega = f + \zeta$. In isopycnal coordinates, Ertel PV is defined as $q = \omega/h$ and using (1) and (3), it satifies the equation

$$\frac{Dq}{Dt} \equiv \frac{\partial q}{\partial t} + \mathbf{u} \cdot \nabla q = 0. \tag{4}$$

Eq. (4) shows that, in the inviscid and adiabatic system, PV is conserved along particle trajectories following the horizontal velocity $\mathbf{u}$, just like a passive tracer.

2.2. Defining an eddy closure on PV

The work in this subsection follows very closely that in Section 1 of Gent et al. (1995). If the variables are decomposed into large-scale components denoted by an overbar and eddy components denoted by primes by a low-pass projection operator in time and space at constant density, then the thickness Eq. (1) becomes

$$\frac{\partial \bar{h}}{\partial t} + \nabla \cdot \left(\bar{h}\bar{\mathbf{u}} + \overline{h'\mathbf{u}'}\right) \equiv \frac{\partial \bar{h}}{\partial t} + \nabla \cdot (\bar{h}\mathbf{U}) = 0. \tag{5}$$

Thus, the layer thickness is transported by the horizontal velocity $\mathbf{U} = \bar{\mathbf{u}} + \mathbf{u}^*$, where $\mathbf{u}^* = \overline{h'\mathbf{u}'}/\bar{h}$ is commonly referred to as the bolus, or eddy-induced, velocity. The precise form of the closure is not required for the analysis below, i.e. the analysis holds for any type of closure that results in the transport velocity $\mathbf{U}$ differing from the mean velocity $\bar{\mathbf{u}}$.

The equation for any large-scale tracer in isopycnal coordinates is derived from the projection of the equation for tracer density, h times the tracer, see Eq. 2 of Gent et al. (1995). When the tracer is the PV, this means projecting (3) for the absolute vorticity to get

$$\frac{\partial \bar{\omega}}{\partial t} + \nabla \cdot (\bar{\omega}\bar{\mathbf{u}} + \overline{\omega'\mathbf{u}'}) = 0. \tag{6}$$

Following the discussion on page 427 of Greatbatch (1998), it is preferable to define the mean PV as the thickness-weighted mean, so that

$$\bar{\omega} = \bar{q}\bar{h}, \omega' = \bar{h}q' + \bar{q}h', \tag{7}$$

then (6) can be rewritten in the form

$$\frac{\partial(\bar{h}\bar{q})}{\partial t} + \nabla \cdot (\bar{h}\bar{q}\bar{\mathbf{u}} + \overline{h'\mathbf{u}'}\bar{q}) = -\nabla \cdot (\bar{h}\overline{q'\mathbf{u}'}). \tag{8}$$

This is the conservative form of the PV equation that leads to the theorems found by Haynes and McIntyre (1987) and Haynes and McIntyre (1990). It is very important to note that ω is a linear function of $\mathbf{u}$, so that the mean relative vorticity, $\bar{\zeta}$, and the mean PV, $\bar{q}$, are both functions of the mean velocity, $\bar{\mathbf{u}}$.

The fundamental assumption now used is that ocean eddies mix PV along isopycnals and not across them, so that the right-hand-side of (8) can be parameterized as Laplacian diffusion along isopycnals with coefficient κ. Then (8) becomes

$$\frac{\partial(\bar{h}\bar{q})}{\partial t} + \nabla \cdot (\bar{h}\bar{q}\mathbf{U}) = \nabla \cdot (\kappa\bar{h}\nabla\bar{q}), \tag{9}$$

where the small-slope approximation has been used in the diffusion term, see Eq. (2) of Gent and McWilliams (1990). Using (5), (9) can be written as an equation for the mean PV as

$$\frac{D^*\bar{q}}{Dt} \equiv \frac{\partial \bar{q}}{\partial t} + \mathbf{U} \cdot \nabla\bar{q} = \frac{\nabla \cdot (\kappa\bar{h}\nabla\bar{q})}{\bar{h}}. \tag{10}$$

Note that this is exactly the equation for an arbitrary tracer given in Eq. (6) of Gent et al. (1995) applied to the mean PV, which is advected by the transport velocity $\mathbf{U}$ and diffused along isopycnal surfaces. Use of this closure for PV has been proposed before, see Eq. (91) of Greatbatch (1998) and Smith (1999). This form of closure is appealing because a momentum equation that is consistent with (10) will retain an analog to Kelvin's circulation theorem where, in the absence of diffusion, potential vorticity is conserved along particle trajectories that follow $\mathbf{U}$.

The standard GM closure modifies the isopycnal layer thickness and the temperature and salinity equations, but it does not change the momentum equation for the mean velocity $\bar{\mathbf{u}}$. It is important to note that a PV closure does change the momentum equation, and an energy analysis and the momentum equation using the closure in (10) will be explored in the next two sections.

3. Analysis of energetics

The momentum equation consistent with the PV closure shown in (9) is

$$\frac{\partial \mathbf{u}}{\partial t} + (f+\zeta)\mathbf{k}\times\mathbf{U} + \nabla\phi + \nabla K' = \mathbf{k}\times(\kappa h \nabla q), \tag{11}$$

where the overbars to represent mean quantities have now been dropped. The PV equation shown in (9) can be derived by taking the curl of (11) and combining the result with (5). Note that the term $(f+\zeta)\mathbf{k}\times\mathbf{U}$ is equivalent to $hq\mathbf{k}\times\mathbf{U}$ and is solely responsible for producing a system in which mean PV is advected by the total velocity $\mathbf{U}$. Eq. (11) includes the gradient of the mean Montgomery potential, ϕ, along with the gradient of an undefined function, K'. We must include K' in (11) since the compatibility between the momentum and PV equations can only be constrained to within the gradient of a potential function. Comparison with (2) suggests that K' should be a form of kinetic energy, and this is explored in the next subsections.

3.1. The unmodified system

The inviscid and adiabatic system given in Section 2.1 does conserve the sum of kinetic and potential energy, defined as total mechanical energy. The total mechanical energy equation results from adding $(K+\phi)*(1)$ and $h\mathbf{u}\cdot(2)$ to obtain

$$\frac{\partial}{\partial t}(hK) + \phi\frac{\partial h}{\partial t} + \nabla\cdot(hK\mathbf{u}) + \nabla\cdot(h\phi\mathbf{u}) = 0. \tag{12}$$

Eq. (12) shows there is a conservative exchange between kinetic and potential energy due to the interaction between the thickness, Montgomery potential (defined following (2)) and the velocity field. Integrating (12) over the entire (x,y,ρ) domain, with suitable boundary conditions on $\mathbf{u}$ and assuming hydrostatic balance, gives the domain-averaged total mechanical energy equation

$$\frac{d}{dt}\int_V \left[hK + \frac{gz^2}{2\rho_0}\right] dx\,dy\,d\rho = 0. \tag{13}$$

Eq. (13) shows that $h\,K + gz^2/2\rho_0$ is a global invariant of the inviscid, Boussinesq and adiabatic system.

3.2. Energetics of the PV eddy closure

The energy relations of the PV eddy closure should mimic those of the unmodified system. In particular, the important physical property that the Coriolis force does not contribute to the KE should be retained, which requires that the dot product of the momentum Eq. (11) is by the total velocity $\mathbf{U}$. Thus, the kinetic energy equation is formed by adding $K' *$ (5) and $h\mathbf{U}\cdot$ (11), but ignoring the mixing term on the RHS of (11), to obtain

$$K'\frac{\partial h}{\partial t} + h\mathbf{U}\cdot\frac{\partial \mathbf{u}}{\partial t} + \nabla\cdot(h\mathbf{U}K') = -h\mathbf{U}\cdot\nabla\phi. \tag{14}$$

Note that the mixing term on the RHS of (11) has been dropped in this inviscid analysis, but will be analysed in the next Section. The total energy equation is constructed by adding (14) and the PE equation, derived by $\phi *$ (5), to yield

$$K'\frac{\partial h}{\partial t} + h\mathbf{U}\cdot\frac{\partial \mathbf{u}}{\partial t} + \phi\frac{\partial h}{\partial t} + \nabla\cdot(h\mathbf{U}K') + \nabla\cdot(h\mathbf{U}\phi) = 0. \tag{15}$$

Note that, as in the unmodified system, the exchange terms from (14) and the PE equation combine to produce a single divergence term that vanishes when integrated over the entire domain. This results from the fact that the same velocity, $\mathbf{U}$, that transports the layer thickness is dotted into the momentum Eq. (11) to form the KE equation.

The complication in deriving the energy relation for the PV eddy closure arises during the consideration of K'. In general, the first two terms of (15) can not be combined because the transport velocity $\mathbf{U}$ differs from the mean velocity $\mathbf{u}$. There is no general definition of K' that makes these terms combine. However, if K' is chosen as

$$K' = \frac{1}{2}(\mathbf{u}\cdot\mathbf{u}) + (\mathbf{u}\cdot\mathbf{u}^*) = \frac{1}{2}(\mathbf{u}\cdot\mathbf{U}) + \frac{1}{2}(\mathbf{u}\cdot\mathbf{u}^*), \tag{16}$$

this results in a total energy equation of the form

$$\frac{\partial}{\partial t}(hK') + \phi\frac{\partial h}{\partial t} + \nabla\cdot(h\mathbf{U}K') + \nabla\cdot(h\phi\mathbf{U}) = h\mathbf{u}\cdot\frac{\partial \mathbf{u}^*}{\partial t}. \tag{17}$$

Thus, the PV eddy closure has an energy relation analogous to the unmodified system, but with an error in total energy conservation proportional to the time derivative of the bolus velocity. We made this choice for K' because it has the usual first term from the mean velocity, and results in only a single RHS term in (17) that is proportional to $\partial\mathbf{u}^*/\partial t$. This term is small because $\mathbf{u}^*$ is small compared to $\mathbf{u}$.

4. The momentum equation

Now that K' has been defined in (16), this completes the form of the PV closure momentum Eq. (11). In this section, properties of the term due to the mixing of PV along isopycnals on the RHS of (11) are explored. Very often the full PV in the mixing term has been replaced by the planetary vorticity, and the relative vorticity component has been ignored. The planetary vorticity component, f/h, on the RHS of (11) produces a zonal momentum equation of the form

$$\frac{\partial u}{\partial t} - (f+\zeta)V + \frac{\partial \phi}{\partial x} + \frac{\partial K'}{\partial x} = -\kappa\beta + \frac{\kappa f h_y}{h}, \tag{18}$$

where u and V are the zonal and meridional components of $\mathbf{u}$ and $\mathbf{U}$, respectively. Note that if the GM form for the bolus velocity is assumed, then the $-fv^*$ term on the LHS cancels the second RHS term in (18). However, we have not assumed the GM form in our analysis, which is general for any choice of the bolus velocity. The $-\kappa\beta$ term on the RHS of (18) has been discussed in many previous papers such as Welander (1973), Treguier et al. (1997), Wardle and Marshall (2000), Zhao and Vallis (2008) and Eden (2010).

The relative vorticity component of PV, ζ/h, on the RHS of (11) produces a zonal momentum equation of the form

$$\frac{\partial u}{\partial t} + \cdots = \kappa(u_{yy} - v_{xy}) + \frac{\kappa\zeta h_y}{h}. \tag{19}$$

The first two terms on the RHS look like viscous terms, especially if the horizontal velocity is nearly nondivergent, so that $-v_{xy} \approx u_{xx}$. However, there are two problems that arise if these terms are considered as the viscosity closure of the model. The first problem with the RHS of (19) is that it cannot be expressed as the divergence of a tensor divided by h. This is the required form in isopycnal coordinates to ensure a positive definite sink of global kinetic energy (Condition I hereafter), e.g. see Smith and McWilliams (2003) and Griffies (2004). The second problem is that the RHS of (19) is derived from a curl operator, which is antisymmetric when written as a stress tensor. Therefore, it cannot satisfy the condition that the viscosity should not affect velocity fields associated with solid body rotation (Condition II hereafter), see Wajsowicz (1993).

Because of these problems, it is not clear to us that a global ocean model based on (11) will remain numerically stable. However, the zonal channel model based on this equation described in Section 5 is numerically stable when using the RHS of (11) as the dissipative closure. If one judges Conditions I and II to be very important properties, the most straightforward way to change the RHS of (19) into a viscous closure that satisfies both Conditions I and II is to approximate it as Laplacian diffusion of u, and to add the necessary Jacobian term. Then the zonal momentum equation becomes

$$\frac{\partial u}{\partial t} + \cdots = \frac{\nabla \cdot (\kappa h \nabla u)}{h} - \frac{J_{xy}(\kappa h, v)}{h}. \tag{20}$$

Note that the KE Eq. (14) is formed by $h\mathbf{U}\cdot$ (11), so that to ensure a sink of KE in this equation, (u, v) on the RHS of (20) should be replaced by (U, V). However, we believe that using the standard viscous closure in terms of (u, v) is more pragmatic. A global model using this viscous closure will be numerically stable because momentum transfer is downgradient. A possible disadvantage of this closure is that momentum transfer is known to be upgradient in ocean jets, such as the Antarctic Circumpolar Current, see McWilliams and Chow (1981).

Retaining the planetary component of PV on the RHS of (11), but changing to the viscous closure that satisfies Conditions I and II, gives the momentum equation as

$$\begin{aligned}\frac{\partial \mathbf{u}}{\partial t} &+ (f+\zeta)\mathbf{k}\times\mathbf{U} + \nabla\phi + \nabla K' \\ &= \kappa h \mathbf{k} \times \nabla\left(\frac{f}{h}\right) + \frac{\nabla\cdot(\kappa h \nabla \mathbf{u})}{h} + \frac{J_{xy}(\kappa h, \mathbf{k}\times\mathbf{u})}{h}.\end{aligned} \tag{21}$$

This is an alternative momentum equation we suggest could be used in ocean models, rather than (11) which resulted directly from the downgradient PV mixing assumption. Using the definition of K' in (16), Eq. (21) can also be written in the form

$$\begin{aligned}\frac{D^*\mathbf{u}}{Dt} &+ \mathbf{u}\cdot\nabla\mathbf{u}^* + f\mathbf{k}\times\mathbf{U} + \nabla\phi = \kappa h \mathbf{k}\times\nabla\left(\frac{f}{h}\right) \\ &+ \frac{\nabla\cdot(\kappa h\nabla\mathbf{u})}{h} + \frac{J_{xy}(\kappa h, \mathbf{k}\times\mathbf{u})}{h}.\end{aligned} \tag{22}$$

The unfamiliar second term on the LHS is a summation over the two components of $\mathbf{u}$ and $\mathbf{u}^*$.

All the equations so far have been written in isopycnal coordinates, but many ocean models use height as the vertical coordinate. The general form of the momentum Eq. (11), with K' defined by (16), transformed into z-coordinates becomes

$$\begin{aligned}\frac{D^*\mathbf{u}}{Dt} &+ \mathbf{u}\cdot\left(\nabla\mathbf{u}^* - \frac{\nabla\rho}{\rho_z}\frac{\partial\mathbf{u}^*}{\partial z}\right) + f\mathbf{k}\times\mathbf{U} + \frac{\nabla p}{\rho_0} \\ &= \kappa\mathbf{k}\times(\nabla q - q_z\nabla\rho\rho_z)/\rho_z.\end{aligned} \tag{23}$$

The gradient operator is now with respect to constant z, and the summation in the bracketed term on the LHS is over the two components of $\mathbf{u}$ and $\mathbf{u}^*$. Eq. (23) has a similar form to the two-dimensional, zonally-averaged momentum equation discussed in Section 8 of Plumb and Ferrari (2005), which only simplifies when the small Rossby number approximation is invoked. However, the momentum Eq. (23) is fully three-dimensional, and there is no approximation used in deducing it from the assumed potential vorticity Eq. (10). Transforming our alternative momentum Eq. (22) into z-coordinates gives

$$\begin{aligned}\frac{D^*\mathbf{u}}{Dt} &+ \mathbf{u}\cdot\left(\nabla\mathbf{u}^* - \frac{\nabla\rho}{\rho_z}\frac{\partial\mathbf{u}^*}{\partial z}\right) + f\mathbf{k}\times\mathbf{U} + \frac{\nabla p}{\rho_0} \\ &= \kappa\mathbf{k}\times\left(\nabla f + f\left(\frac{\nabla\rho}{\rho_z}\right)_z\right) + \nabla\cdot(\kappa\nabla\mathbf{u}) + J_{xy}(\kappa, \mathbf{k}\times\mathbf{u}).\end{aligned} \tag{24}$$

Note that the density gradient terms arising from the transformation of the viscous terms in (22) have been ignored, so that the viscous terms in (24) are the standard form in z-coordinates, which includes the Jacobian term when κ is variable, see Wajsowicz (1993). Eqs. (23) and (24) contain terms proportional to the density slope and its vertical derivative, so they might have to be tapered in the mixed layer where the slopes become steep.

5. Evaluation of PV closures

In order to better understand the attributes of the various approaches to PV closure, we conduct a set of re-entrant channel simulations that loosely follows the geometry used by McWilliams and Chow (1981). The system configuration is meant to serve as an idealized model of the Antarctic Circumpolar Current. As discussed below, our motivation for choosing this configuration is that channel dynamics are particularly challenging for eddy parameterizations. Our purpose is not to complete a tuning exercise where we attempt to obtain a best-fit with eddying solutions, rather our goal is to compare, contrast and, hopefully, better understand a few of the tenable approaches that modify mean PV through the parameterization of eddy processes.

The numerical model is configured in a 2000 km $\times$ 2000 km domain that is periodic in the zonal direction and bounded in the meridional direction with no-slip boundary conditions. The β-plane approximation is used with $f_0 = -1.1\times10^{-4}\,\mathrm{s}^{-1}$ and $\beta = 1.4\times10^{-11}\,\mathrm{m}^{-1}\,\mathrm{s}^{-1}$. The simulations include three isopycnal layers with mean layer thicknesses of 500 m, 1250 m and 3250 m with densities of 1010 kg m^{-3},1013 kg m^{-3} and 1016 kg m^{-3}, respectively. The system is forced by a zonal wind stress applied to the top model layer of the form $\tau = \tau_0 e^{(y-y_0/r)^2}$ where $\tau_0 = 0.1\,\mathrm{N\,m}^{-2}$, y_0 is the meridional mid-point of the channel and r = 300 km. As shown below, the jet region is far removed from the lateral boundaries to better simulate the dynamics of an unconstrained zonal jet.

The model used in this study is based on the C-grid numerical scheme presented in Thuburn et al. (2009) and Ringler et al. (2010). This numerical method is being used to develop global atmosphere and ocean models as a part of the Model for Prediction Across Scales (MPAS) project. The MPAS modeling approach is attractive for this study because potential vorticity is conserved to within machine precision, i.e. we retain Kelvin's circulation theorem in the numerical model to within machine precision. As a result, we can implement (11), either in its entirety or by selectively choosing specific components of the PV closure, while still conserving mean PV in the numerical model.

As summarized in Table 1, four model configurations are discussed. The first configuration serves as the high-resolution reference solution (referred to hereafter as REF). REF has a resolution of dx = 10 km. Since this resolution is sufficient to resolve the Rossby radius of deformation of the first baroclinic mode that is estimated to be approximately 100 km, no eddy-closure is included in REF. This simulation includes only a $\nu\nabla^4\mathbf{u}$ term on the RHS of the momentum equation with $\nu = 2.0\times10^9\,\mathrm{m}^4\,\mathrm{s}^{-1}$ to remove the downscale cascade of energy and potential enstrophy.

The other three model configurations test various forms of eddy closure, and all use a resolution of dx = 62.5 km. These simulations are meant to represent typical model resolutions that occur in the Southern Ocean when conducting global climate change simulations. The first of these low-resolution experiments uses the

Table 1
REF denotes the high-resolution reference solution that includes no eddy closure. GMST refers to the standard implementation of GM where the momentum equation is unaltered by the eddy closure. PVBL includes the bolus transport part of the GM closure on PV, but omits the isopycnal diffusion of PV. GMPV modifies the momentum equation so that PV is transported by the bolus velocity and diffused along isopycnals. The bolus velocity is computed based on the eddy closure parameter, κ_h, that is set to 500 $m^2\,s^{-1}$. The diffusion of PV in the GMPV simulation is controlled by the value of κ_q. When $\kappa_q = \kappa_h$, PV is treated exactly the same as tracers in the standard implementation of GM. We conduct simulations with κ_q equal to 500 $m^2\,s^{-1}$ and 250 $m^2\,s^{-1}$. The other diffusion parameters are specified as $\nu = 2.0 \times 10^9\ m^4\,s^{-1}$ and $\mu = 1.0 \times 10^2\ m^2\,s^{-1}$.

Simulation	thickness equation	momentum equation
REF	$\frac{\partial h}{\partial t} + \nabla \cdot (h\mathbf{u}) = 0$	$\frac{\partial \mathbf{u}}{\partial t} + (f+\zeta)\mathbf{k} \times \mathbf{u} + \nabla\phi + \nabla K = -\nu\nabla^4\mathbf{u}$
GMST	$\frac{\partial h}{\partial t} + \nabla \cdot (h\mathbf{U}) = 0$	$\frac{\partial \mathbf{u}}{\partial t} + (f+\zeta)\mathbf{k} \times \mathbf{u} + \nabla\phi + \nabla K = \mu\nabla^2\mathbf{u}$
PVBL	$\frac{\partial h}{\partial t} + \nabla \cdot (h\mathbf{U}) = 0$	$\frac{\partial \mathbf{u}}{\partial t} + (f+\zeta)\mathbf{k} \times \mathbf{U} + \nabla\phi + \nabla K' = \mu\nabla^2\mathbf{u}$
GMPV	$\frac{\partial h}{\partial t} + \nabla \cdot (h\mathbf{U}) = 0$	$\frac{\partial \mathbf{u}}{\partial t} + (f+\zeta)\mathbf{k} \times \mathbf{U} + \nabla\phi + \nabla K' = \mathbf{k} \times (\kappa_q h \nabla q)$

standard GM closure (GMST) where the bolus velocity is included in the transport of thickness along with the unmodified momentum equation. The second low-resolution configuration includes the bolus velocity in the transport of PV, but omits the RHS diffusivity of PV (PVBL). Both the GMST and PVBL simulations use a $\mu \nabla^2\mathbf{u}$ as the RHS dissipation with $\mu = 100\ m^2\,s^{-1}$. The third low-resolution configuration modifies the momentum equation such that PV is treated in exactly the same manner as tracers in the GMST system (GMPV); mean PV is transported by the mean plus bolus velocities and is diffused along isopycnals. As discussed below, in the GMPV configuration we explore the scenario where the closure parameter for computing the RHS diffusion of PV (κ_q) differs from the closure parameter used to compute the bolus velocity (κ_h).

Each simulation is run for 8000 days starting from a state of rest with noise added to the mean thickness fields. The noise is included to seed baroclinic instability. All statistics are generated from the last 4000 days of the simulation. Data is sampled every 4 days. The time stepping algorithm is 4th-order Runge Kutta with fully explicit time integration.

The reference solution evolves into turbulent motion at about day 1200 of the simulation. A snapshot of the PV field at day 6000 is shown in Fig. 1. The system is characterized by a meandering jet that sheds PV filaments in both the equatorward and poleward directions. These PV filaments occlude to become long-lived, coherent vortical features moving in the opposite direction from the zonal jet. The spectrum of the kinetic energy field along the $y = y_0$ line (not shown) shows a slope very close to -3 that is indicative of fully-developed, geostrophic turbulence (Vallis, 2006).

The primary goal of eddy parameterization is to mimic the eddy-induced fluxes of layer thickness, tracers, potential vorticity and/or momentum based on the large-scale structure. We present in Fig. 2 the zonal-mean, time-mean meridional eddy fluxes of thickness, potential vorticity and momentum that occur in the top layer of the eddy-resolving reference simulation. Each figure panel also contains the zonal-mean, time-mean field that is impacted through the meridional convergence of these eddy-fluxes. Panel A shows that the eddy-induced thickness flux, $\overline{h'v'}$, is negative (poleward) across the jet region. Similarly, panel B indicates that the eddy-induced potential vorticity flux, $\overline{(hv)'q'}$, is also poleward in the jet. The meridional gradients in mean thickness and mean PV are positive throughout the region of the jet. Thus, the

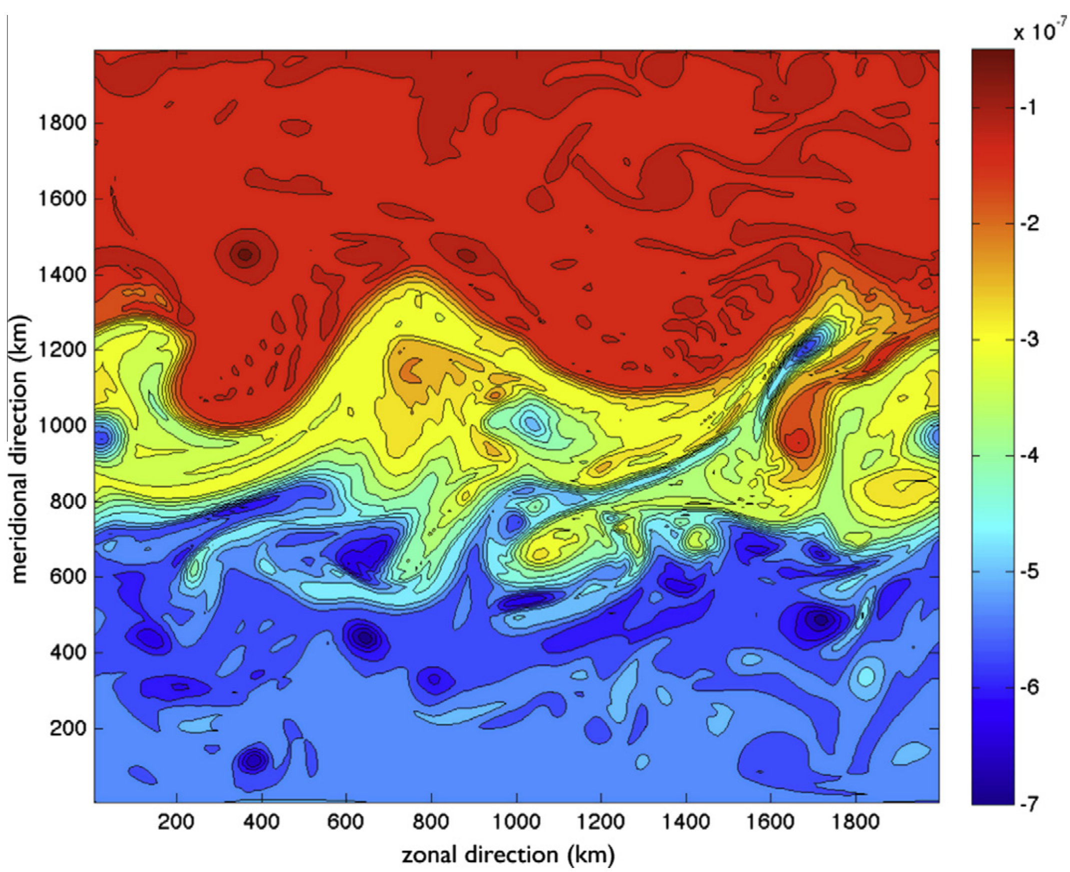

Fig. 1. A snapshot of PV in the upper ocean layer at day 6000 from the reference simulation. Strong PV gradients exist along the core of the meandering jet. PV filaments are shed, resulting in occluded PV cores that, on average, slowly propagate to the west.

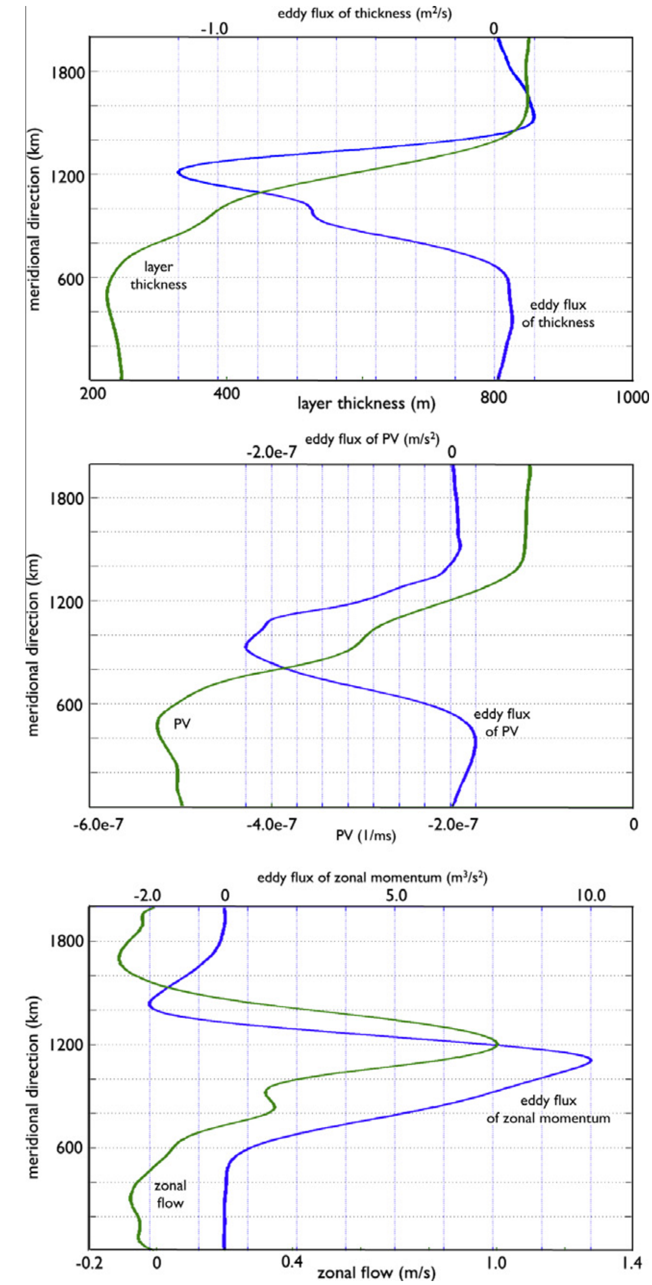

Fig. 2. All panels show eddy flux and mean state for the upper ocean layer. Panel A: The eddy-induced meridional flux of thickness, $\overline{v'h'}$, along with the zonal-mean, time-mean thickness field. Panel B: The eddy-induced meridional flux of potential vorticity, $\overline{(hv)'q'}$, along with the zonal-mean, time-mean potential vorticity field. Panel C: The eddy-induced meridional flux of momentum, $\overline{(hv)'u'}$, along with the zonal-mean, time-mean zonal wind field.

eddy-induced fluxes of thickness and potential vorticity are *down-gradient*. Panel C shows that the eddy-induced momentum flux, $\overline{(hv)'u'}$, is qualitatively very different. On the equatorward side of the jet, the eddy-induced momentum fluxes are weakly negative (poleward) and are directed up the gradient of zonal flow. On the poleward flank of the jet, the eddy-induced momentum fluxes are strongly positive (equatorward) and are also directed up the gradient of zonal flow. As a result, the eddy-induced momentum fluxes act to accelerate the mean zonal jet.

Using the approach detailed in McWilliams and Chow (1981), these eddy fluxes can be combined with the gradients of the mean fields to calculate an effective diffusion of the mean fields by the eddies, i.e. we can compute how effective the eddies are at modifying the large-scale, mean fields. We compute the effective diffusivity of layer thickness, κ_h, by estimating $\kappa_h = -\overline{h'v'}/\frac{\partial \bar{h}}{\partial y}$ throughout the jet region. While the diffusivities tend to be noisy, we estimate a mean value of κ_h to be roughly 500 $m^2\,s^{-1}$ averaged across the jet. In all eddy-closure simulations we compute the bolus velocity as $\mathbf{u}^* = -\kappa_h \nabla \bar{h}/\bar{h}$ with κ_h = 500 $m^2\,s^{-1}$. The effective diffusivity of PV is determined by estimating $-\overline{(hv)'q'}/\left(\bar{h}\frac{\partial \bar{q}}{\partial y}\right)$ to be roughly 500 $m^2\,s^{-1}$, which is the same magnitude as the layer thickness diffusivity. However, the effective diffusivity of momentum varies substantially across the jet region. By estimating $-\overline{(hv)'u'}/\left(\bar{h}\frac{\partial \bar{u}}{\partial y}\right)$ we find values in the neighborhood of -5000 m^2 s^{-1} along the poleward flank of the zonal jet.

The reference simulation is consistent with the results in McWilliams and Chow (1981). The eddies act to smooth the PV gradient through a *down-gradient* flux of eddy-transported PV. Through Kelvin's circulation theorem, this down-gradient flux of PV acts to decelerate the zonal jet. At the same time, the eddies act to accelerate the zonal jet through a *counter-gradient* flux of momentum. Furthermore, the diffusivities obtained in the reference solution are broadly consistent with those shown in Figs. 11, 12 and 13 of McWilliams and Chow (1981). The challenge for the eddy closures discussed below is to mimic these opposing influences on the zonal flow.

The PV field at day 6000 from each of the low-resolution simulations is shown in Fig. 3. The color scale for these figures is identical to that used in Fig. 1. None of the simulations evolve into a steady-state; each has some level of transient wave activity. Of the four simulations, the PVBL has highest level of eddy activity, which develops into a weak turbulent flow. The GMPV simulation with κ_q = 500 $m^2\,s^{-1}$ shows the lowest level of eddy activity with the presence of low-amplitude, highly regular waves propagating along the gradient of PV. The GMST and GMPV with κ_q = 250 $m^2\,s^{-1}$ simulations fall in the middle of the four simulations in terms of their eddy activity.

The low-resolution simulations are evaluated in terms of their time-mean, zonal-mean representation of zonal flow and PV. Fig. 4 shows the time-mean, zonal-mean zonal flow (hereafter, zonal flow) in all three ocean layers for REF and the four low-resolution simulations. Fig. 5 shows the time-mean, zonal-mean PV field (hereafter, PV field) for the same set of simulations.

The reference solution has a zonal jet of approximately 1.0 $m\,s^{-1}$ in the top model layer that is shifted approximately 200 km equatorward of mid-channel. The characteristic width of the jet is commensurate with the half-width of the wind stress. Outside the jet region, there is essentially no zonal flow. The lowest layer exhibits a jet that is slightly broader and about 40% as strong as the jet in the top layer. In terms of PV, REF shows a linear gradient across the top-layer jet region that is in near-geostrophic balance with the zonal flow. The PV gradient in the top layer is dominated by the gradient of h, with β and ζ playing secondary roles. Outside the jet region, PV shows little variation in the meridional direction. In the middle layer, the eddy-resolving simulation has almost completely mixed PV. A weak reversal of the PV gradient is produced in the bottom layer. In the region of the jet, the PV gradient in the bottom layer is two orders of magnitude smaller than that found in the top layer.

The standard GM simulation does not evolve into fully-developed turbulence; the transfer of available potential energy to unresolved scales by the closure suppresses the instability in the jet region. GMST largely reproduces the reference simulation. Throughout all model layers, GMST exhibits a jet that is slightly weaker, broader and shifted 200 km poleward relative to REF. GMST does not do as well with respect to the mean PV fields. While

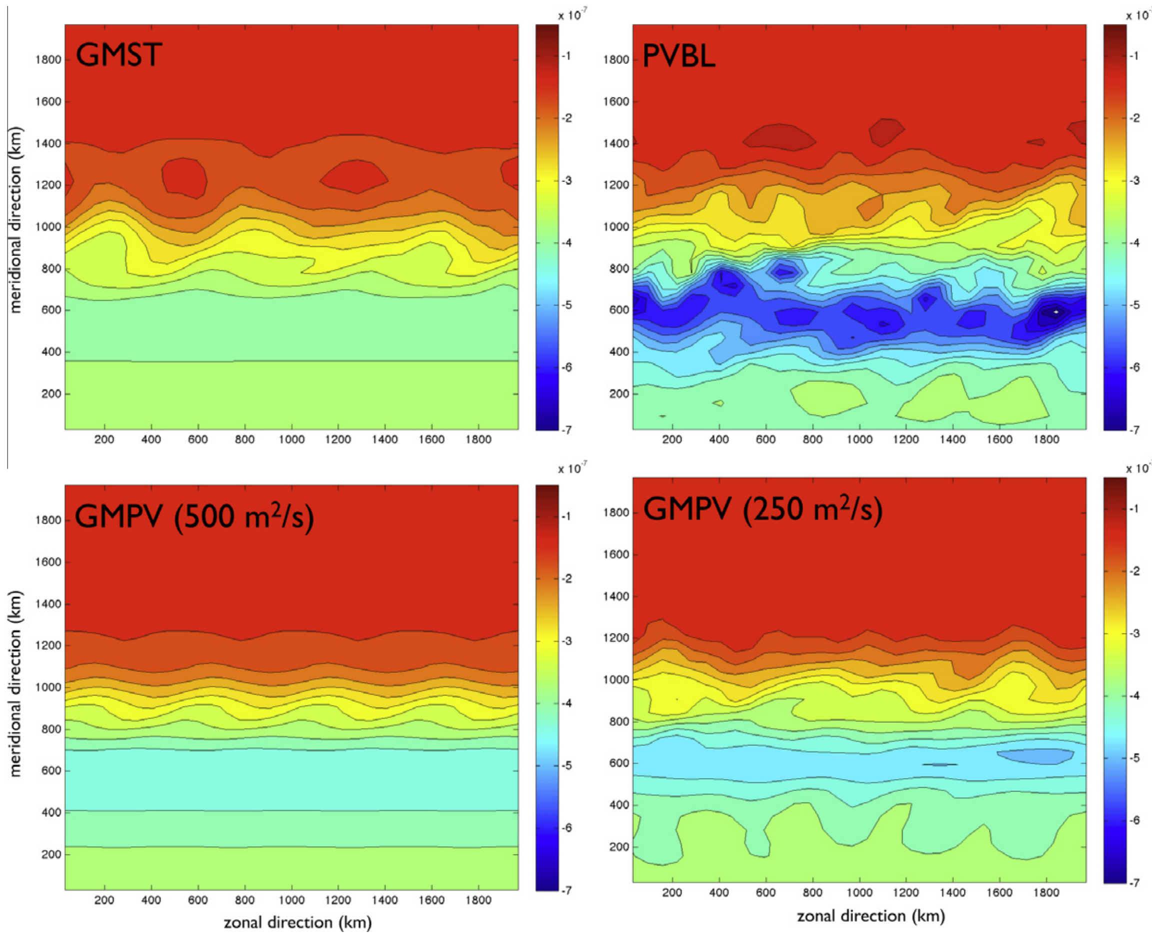

Fig. 3. A snapshot of PV in the upper ocean layer at day 6000 from the four simulations that include an eddy-closure.

none of the eddy-closure simulations capture the structure of the top-layer PV field on the poleward side of the jet in the REF simulation, GMST produces the weakest overall PV gradient. In the middle layer, GMST shows the least ability to thoroughly mix PV, as found in the REF simulation.

We find that altering the GMST configuration by simply including the bolus term in PV transport (PVBL) leads to relatively large changes. Including the transport of PV by the bolus velocity leads to an exact exchange between potential and kinetic energy. As a result, the potential energy that is removed in the GMST simulation is transfered into zonal kinetic energy in the PVBL simulation leading to an acceleration of the jet. The PVBL experiment does evolve into turbulence. The acceleration of the zonal jet via the bolus transport of PV acts to instigate a baroclinic instability in the jet region. In terms of the zonal flow, PVBL is very similar to GMST except shifted 300 km equatorward. In terms of the PV field, PVBL is markedly different than GMST. Overall, PVBL more closely than any other of the closure simulations reproduces the REF PV field in all layers.

Certainly in terms of the zonal flow, GMPV with $\kappa_q = 500\ \mathrm{m^2\ s^{-1}}$ is the least satisfactory of the eddy-closure simulations. Recall that since $\kappa_q = \kappa_h$, this simulation treats PV in exactly the same way as GMST treats tracers. This simulation produces the weakest zonal jet that is displaced the farthest from the REF solution. Outside of the core jet region, GMPV with $\kappa_q = 500\ \mathrm{m^2\ s^{-1}}$ produces westward jets of approximately 0.3 m $\mathrm{s^{-1}}$ that are not seen in the REF simulation. In the region of westward flow, the meridional gradient of thickness is small and the PV gradient is due, primarily, to β. The $-\kappa\beta$ term in (18) of the PV diffusion term produces a constant westward acceleration at every location in the domain. This westward bias in the flow is clearly evident in all model layers. In terms of the PV field, GMPV with $\kappa_q = 500\ \mathrm{m^2\ s^{-1}}$ is not particularly notable by producing errors that are larger than PVBL but smaller than GMST.

Given that the GMPV simulation with $\kappa_q = 500\ \mathrm{m^2\ s^{-1}}$ is clearly deficient, we explore using a smaller value for κ_q than for κ_h. While there is no theoretical justification for doing this, we hope it might provide insights into paths forward. The last simulation we discuss is GMPV with $\kappa_q = 250\ \mathrm{m^2\ s^{-1}}$ (see footnote[1]). This reduction in κ_q results in a better representation of the REF solution in every respect. Reducing κ_q from 500 $\mathrm{m^2\ s^{-1}}$ to 250 $\mathrm{m^2\ s^{-1}}$ leads to a stronger zonal jet positioned much closer to that found in the REF simulation. In addition, the spurious westward flow is reduced, if only slightly. In terms of the reproducing the PV field from REF, the reduction in κ_q results in more modest improvements. For example, the $\kappa_q = 250\ \mathrm{m^2\ s^{-1}}$ simulations does slightly better than the $\kappa_q = 500\ \mathrm{m^2\ s^{-1}}$ simulation in capturing the PV gradient in the top layer.

In terms of representing the jet region, GMPV with $\kappa_q = 250\ \mathrm{m^2\ s^{-1}}$ is arguably, if only marginally, better than the GMST or PVBL simulations. Yet outside the jet region the GMPV simulations show a strong westward bias. In the section below we discuss possible remedies to remove this strong westward bias.

[1] In many respects it makes more sense to reduce κ_q to 100 $\mathrm{m^2\ s^{-1}}$ to match the value of μ used in the GMST and PVBL simulations. It turns out that the GMPV simulation is unstable with $\kappa_q = 100\ \mathrm{m^2\ s^{-1}}$ unless we include a small amount of additional dissipation in the form of $\nabla^2\mathbf{u}$ or $\nabla^4\mathbf{u}$.

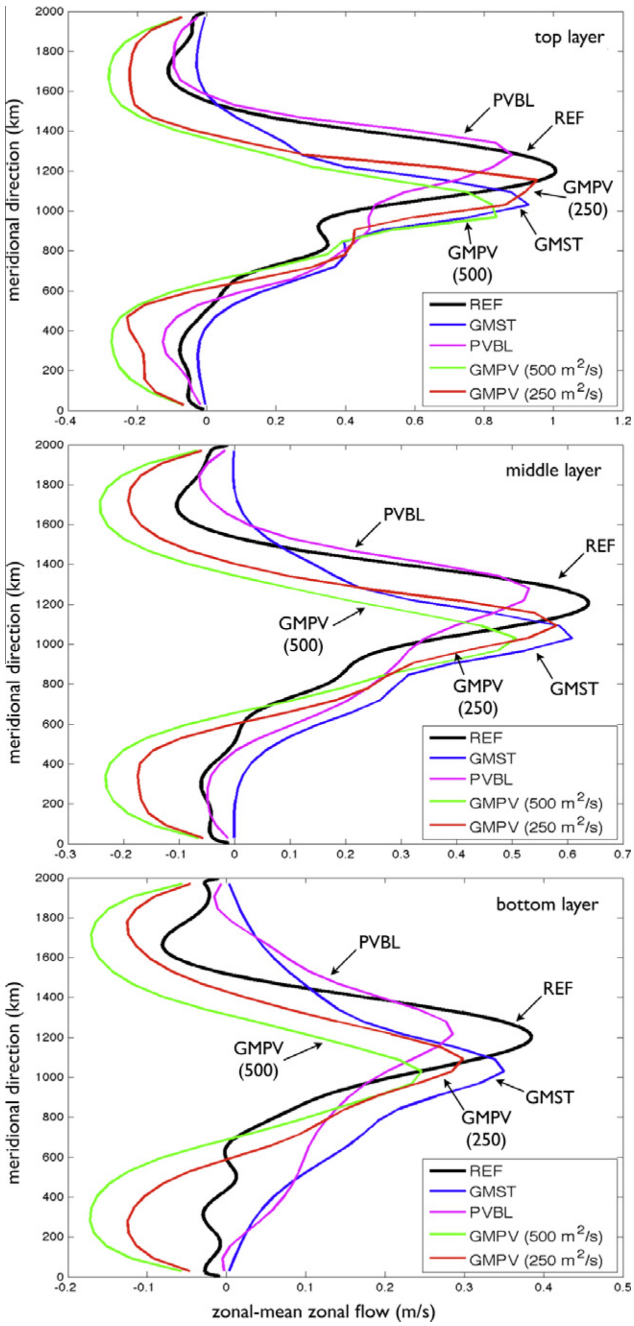

Fig. 4. Zonal-mean, time-mean zonal flow for the reference solution and four simulations that use different forms of eddy-closure.

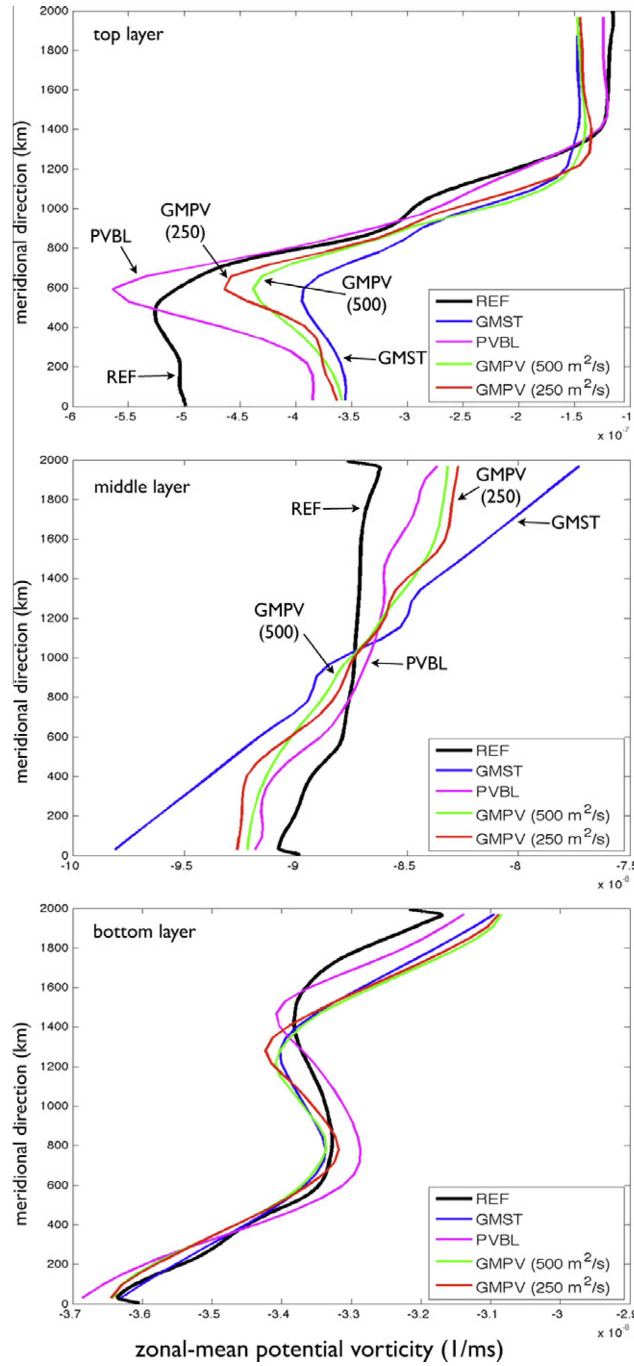

Fig. 5. Zonal-mean, time-mean PV for the reference solution and four simulations that use different forms of eddy-closure.

6. Discussion and conclusions

There are three main conclusions from the theoretical part of this paper where we have formulated in isopycnal coordinates an eddy closure for Ertel potential vorticity that is identical to that for passive tracers.

The first is that treating PV exactly like any passive tracer in isopycnal coordinates leads to the mean PV being a function of the mean velocity. In turn, this leads to the PV closure having a momentum equation to predict the mean velocity. In addition, this momentum equation is not unique because it contains the gradient of an undefined potential function. This non-uniqueness has been noted before on page 430 of Greatbatch (1998), and Eq. (75) of Smith (1999) also contains the gradient of an undefined potential function. This undefined potential function does not project into the rotational component of the velocity field, but rather projects entirely into the divergent component of the velocity field. The divergent component of the velocity field plays an important role in the flow of energy through the system, primarily through the storage and release of available potential energy. We use the total energy equation to optimally choose the form of this potential function. When the momentum equation is written in vector invariant form, it becomes apparent that this potential function is related to kinetic energy.

Second, for an arbitrary relationship between the mean and transport velocities it can be shown that the inviscid form of this momentum equation and the thickness equation do not possess an exact conservation property for domain-averaged total energy. The difficulty in the analysis of the energetics arises in the formulation of the kinetic energy. The form of the kinetic energy is not obvious, and the choice in (16) was made because it makes the non-conservation as small as possible since it is proportional to $\partial \mathbf{u}^*/\partial t$. Regardless of the relationship between the mean and transport velocities, momentum equations that are derived from (10) will retain an analog to Kelvin's circulation theorem where, in the absence of diffusion, potential vorticity is conserved along particle trajectories that follow **U**.

Third, the mixing of the relative vorticity part of the PV along isopycnals leads to terms that look like a viscous stress, but these terms do not satisfy two important properties that are usually required of a viscous closure. They do not assure a positive definite sink of global kinetic energy, and they do affect velocity fields associated with solid body rotation. This PV closure also clearly shows that the horizontal viscosity coefficient used in the momentum equation is the same as the along isopycnal mixing coefficient. Very often this is chosen to be equal to the GM closure coefficient κ. This is very unfamiliar, however, because in all implementations of the GM scheme that we are aware of, the viscosity coefficient has always been chosen with different criteria and numerical values than the GM coefficient.

The original GM choice of $\mathbf{u}^*$ assured a domain-averaged sink of potential energy. Gent and McWilliams (1996) show that there is not a PV conservation with the original GM. This paper proposes an eddy closure that extends Gent and McWilliams (1996) to include PV conservation. When the mean and transport velocities are related through the standard GM bolus velocity, the closure includes a non-conservation in total energy; this non-conservation arises because our form of kinetic energy is not conserved along particle trajectories following the transport velocity. The practical implications of this non-conservation of energy need to be carefully evaluated.

The obvious question is whether there are other closure equations that have well defined energy and PV conservation properties? We know of two such equation sets. The first is if the LHS of the momentum equation takes the usual form shown in (2), but with **u** replaced by **U** everywhere, which was first suggested by McDougall and McIntosh (1996) and Greatbatch (1998). However, this implies that the PV is a function of **U**, which, as concluded above, is *not* consistent with assuming a closure in isopycnal coordinates that treats PV exactly like any passive tracer. Never-the-less, "residual-mean" ocean numerical models based on this momentum equation have been built, and global and midlatitude simulations are described in Ferreira and Marshall (2006), and Zhao and Vallis (2008), respectively.

The second such equation set is the Lagrangian-Averaged Navier Stokes (LANS) closure, see Holm (1999). In the LANS closure, there are also two velocities; a transport velocity, called the "smooth velocity", and a predicted mean velocity, called the "rough velocity." The momentum Eq. (11) has essentially the same functional form as the LANS closure when expressed in vector-invariant form, see Eq. (1.4) in Gibbon and Holm (2006). In fact, the *only* differences between this PV eddy closure and the LANS closure is the definition of the potential on the LHS of (11), and the relationship between the transport velocity **U** and the mean velocity **u**, i.e. the specification of $\mathbf{u}^*$. In the GM closure, $\mathbf{u}^*$ is specified to produce a sink of available mean potential energy, whereas in the LANS closure the specification of $\mathbf{u}^*$ is purely kinematic in nature, being only a function of the mean velocity and a single specified parameter called α. Both the LANS closure and our PV eddy closure lead to exact conservation of PV along trajectories defined by the transport velocity **U**, and have unfamiliar terms in the momentum equation like the second term on the LHS of (22). It would be informative to explore further the implications of this striking resemblance between these two closures.

The numerical simulations in a zonal channel clearly suggest that a literal implementation of the PV closure is not appropriate, at least when specifying a globally uniform closure parameter. The issue is not with the bolus transport of PV, but rather with the diffusion of PV. PV differs from tracers in the sense that it is impossible to completely mix PV within isopycnal layers due to the inclusion of planetary vorticity. The westward flow along the flanks of the jet in the GMPV simulations exhibit this difference; the westward flow arises due to the $-\kappa\beta$ term in (18) trying to mix planetary vorticity down-gradient. Obviously, since the eddy closure parameter embodies the mixing that is being parameterized in the non-eddy resolving simulations, where there is no mixing the closure parameter should be near zero. We did not take the next step to allow κ to vary in space, but this will certainly be required if a closure of this type is to be used in practice. Very recently, Eden (2010) has used a κ that varies with y, and has shown that it is vital to retain this "beta" term in order to reproduce idealized channel quasigeostrophic eddy-resolving simulations in a two-dimensional zonally-averaged model with parameterized eddies.

The numerical simulations demonstrate that the GMPV closure approach developed here is viable in the sense that it produces stable solutions. Our conjecture is that the deficiencies in the GMPV simulations can be remedied through the specification of $\kappa = \kappa(y,z)$ for this channel problem. The notable feature of the GMPV closure is that it includes a mechanism that mimics the counter-gradient momentum transport that is found in the eddy-resolving simulations but is missing from GM. This mechanism is obtained through the transport of PV by the bolus velocity.

It is important to note that in the GMPV simulations, the PV closure does contribute to the global momentum budget. It was

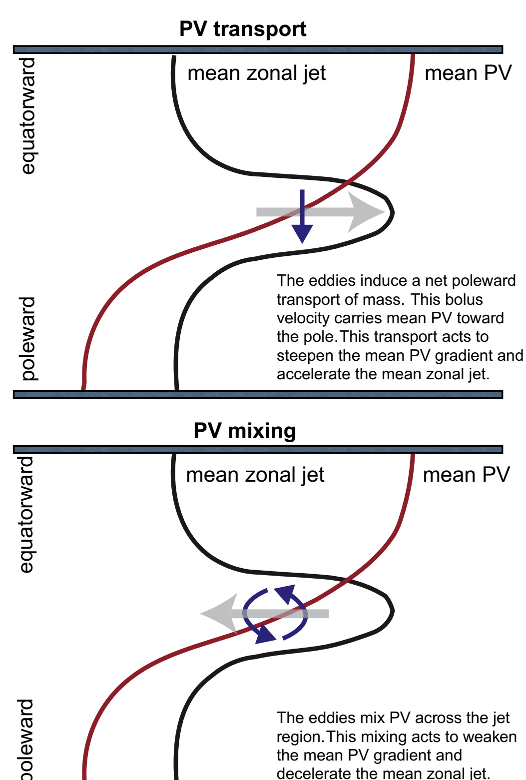

Fig. 6. A conceptual model of how the PV closure acts to modify the zonal flow in the top layer.

pointed out by Green (1970), Welander (1973), and Killworth (1997) that a parameterization in the momentum equation probably should not do so. The simplest way to implement this is to subtract the global integral of the first term from the RHS of (21) or (22). This constraint is the reason that Eden (2010) introduces a gauge term in the forcing, which is defined by the global domain integral of the parameterized forcing in his Eq. (10). However, implementing this constraint changes the kinetic energy equation, and further work is required in order to understand all the consequences of using, or not using, this global constraint.

We conclude with a conceptual model of the how the GMPV closure proposed here alters the PV dynamics of a non-eddy resolving simulation. The conceptual model closely follows the results of Plumb (1979) who showed that eddies act in both an advective and diffusive manner to alter the mean state. As shown in Fig. 6, the proposed PV closure acts to modify the top-layer zonal jet in two ways. First, the transport of PV by the bolus velocity acts to accelerate the eastward jet. Second, the PV closure includes a down-gradient diffusion of PV that acts to mix PV and decelerate the jet. Thus, the PV closure results in two additional forces in the momentum equation that act to push the jet in opposite directions. The opposing forces included in our GMPV closure are in strong analogy to the eddy-induced forces produced in the eddy-resolving, reference simulation. Eddies in the reference solution act to accelerate the zonal flow through the counter-gradient transport of momentum while also acting to decelerate the zonal flow through the down-gradient transport of PV. Looking forward, our challenge is to better measure the effective diffusivity as it varies in space and time, and to further investigate the precise form of diffusion that occurs on the RHS of the momentum equation.

Acknowledgements

The authors thank John Dukowicz, Baylor Fox-Kemper and Matthew Hecht for comments on an early draft of this paper. David Marshall and Geoff Vallis provided many very relevant review comments, which greatly improved the presentation and completeness of the final version. This work was supported by the DOE Office of Science's Climate Change Prediction Program DOE 07SCPF152. NCAR is sponsored by the National Science Foundation.

References

Eden, C., 2010. Parameterising meso-scale eddy momentum fluxes based on potential vorticity mixing and a gauge term. Ocean Modell. 32, 58–71.
Ferreira, D., Marshall, J., 2006. Formulation and implementation of a "residual-mean" ocean circulation model. Ocean Modell. 13, 86–107.
Gent, P.R., McWilliams, J., 1990. Isopycnal mixing in ocean circulation models. J. Phys. Oceanogr. 20, 150–155.
Gent, P.R., McWilliams, J., 1996. Eliassen–Palm fluxes and the momentum equation in non-eddy-resolving ocean circulation models. J. Phys. Oceanogr. 26 (11), 2539–2546.
Gent, P.R., Willebrand, J., McDougall, T., McWilliams, J., 1995. Parameterizing eddy-induced tracer transports in ocean circulation models. J. Phys. Oceanogr. 25, 463–474.
Gibbon, J., Holm, D., 2006. Length-scale estimates for the LANS-α equations in terms of the Reynolds number. Phys. D: Nonlinear Phenom. 220 (1), 69–78.
Greatbatch, R., 1998. Exploring the relationship between eddy-induced transport velocity, vertical momentum transfer, and the isopycnal flux of potential vorticity. J. Phys. Oceanogr. 28 (3), 422–432.
Green, J., 1970. Transfer properties of the large-scale eddies and the general circulation of the atmosphere. Quart. Jour. Royal Met. Soc. 96, 157–185.
Griffies, S.M., 2004. Fundamentals of Ocean Climate Models. Princeton Unversity Press. 496.
Haynes, P., McIntyre, M., 1987. On the evolution of vorticity and potential vorticity in the presence of diabetic heating and frictional or other forces. J. Atmos. Sci. 44, 828–841.
Haynes, P., McIntyre, M., 1990. On the conservation and impermeability theorems for potential vorticity. J. Atmos. Sci. 47, 2021–2031.
Holm, D., 1999. Fluctuation effects on 3D Lagrangian mean and Eulerian mean fluid motion. Phys. D: Nonlinear Phenom. 133 (1–4), 215–269.
Killworth, P., 1997. On the parameterization of eddy transfer Part I. theory. J. Mar. Res. 55 (6), 1171–1197.
Marshall, D., Adcroft, A., 2010. Parameterization of ocean eddies: potential vorticity mixing, energetics and Arnold's first stability theorem. Ocean Modell. 32, 188–204.
Marshall, D., Williams, R., Lee, M., 1999. The relation between eddy-induced transport and isopycnic gradients of potential vorticity. J. Phys. Oceanogr. 29, 1571–1578.
Marshall, J., 1981. On the parameterization of geostrophic eddies in the ocean. J. Phys. Oceanogr. 11, 257–271.
McDougall, T., McIntosh, P., 1996. The temporal-residual-mean velocity. Part I: Derivation and the scalar conservation. J. Phys. Oceanogr. 26, 2653–2665.
McWilliams, J., Chow, J., 1981. Equilibrium geostrophic turbulence I: a reference solution in a beta-plane channel. J. Phys. Oceanogr 11, 921–949.
Plumb, R.A., 1979. Eddy fluxes of conserved quantities by small-amplitude waves. J. Atmos. Sci. 36, 1699–1704.
Plumb, R.A., Ferrari, R., 2005. Transformed Eulerian-mean theory. Part I: nonquasigeostrophic theory for eddies on a zonal-mean flow. J. Phys. Oceanogr. 35, 165–174.
Rhines, P., Young, W., 1982. Homogenization of potential vorticity in planetary gyres. J. Fluid Mech. 122, 347–367.
Ringler, T., Thuburn, J., Klemp, J., Skamarock, W., 2010. A unified approach to energy conservation and potential vorticity dynamics for arbitrarily-structured c-grids. J. Comput. Phys. 229 (1), 3065–3090.
Smith, R., 1999. The primitive equations in the stochastic theory of adiabatic stratified turbulence. J. Phys. Oceanogr. 29 (8), 1865–1880.
Smith, R., McWilliams, J., 2003. Anisotropic horizontal viscosity for ocean models. Ocean Modell. 5 (2), 129–156.
Thuburn, J., Ringler, T., Klemp, J., Skamarock, W., 2009. Numerical treatment of geostrophic modes on arbitrarily structured c-grids. J. Comput. Phys. 228, 8321–8335.
Treguier, A., Held, I., Larichev, V., 1997. Parameterization of quasigeostrophic eddies in primitive equation ocean models. J. Phys. Oceanogr. 27, 567–580.
Vallis, G.K., 2006. Atmospheric and Oceanic Fluid Dynamics. Cambridge University Press, Cambridge, U.K.. pp. 745.
Wajsowicz, R., 1993. A consistent formulation of the anisotropic stress tensor for use in models of the large-scale ocean circulation. J. Comput. Phys. 105, 333–338.
Wardle, R., Marshall, J., 2000. Representation of eddies in primitive equation models by a pv flux. J. Phys. Oceanogr. 30, 2481–2503.
Welander, P., 1973. Lateral friction in the oceans as an effect of potential vorticity mixing. Geophys. &Astrophys. Fluid Dyn. 5 (1), 173–189.
Zhao, R., Vallis, G., 2008. Parameterizing mesoscale eddies with residual and Eulerian schemes, and a comparison with eddy-permitting models. Ocean Modell. 23 (1–2), 1–12.